

Design and Simulation of Low Speed Axial Flux Permanent Magnet (AFPM) Machine

Hassan Moradi¹, Ahmad Darabi²

¹Faculty of Electrical & Robotic Engineering, Shahrood University of Technology

²Faculty of Electrical & Robotic Engineering, Shahrood University of Technology
(¹hassanmoradi333@yahoo.com, ²Darabi_Ahmad@hotmail.com)

Abstract-In this paper presented initial design of Low Speed Axial Flux Permanent Magnet (AFPM) Machine with Non-Slotted TORUS topology type by use of certain algorithm (Appendix). Validation of design algorithm studied by means of selected data of an initial prototype machine. Analytically design calculation carried out by means of design algorithm and obtained results compared with results of Finite Element Method (FEM).

Keywords- Axial Flux Permanent Magnet (AFPM) Machine; Design Algorithm; Finite Element Method (FEM); TORUS.

I. INTRODUCTION

The first work focused on PM disc machines was performed in late 70s and early 80s. Disc type axial flux PM machines have found growing interests in the last decade especially in the 90s and have been increasingly used in both naval and domestic applications as an attractive alternative to conventional radial flux machines due to its pancake shape, compact construction and high power density [1], [2].

AFPM motors are particularly suitable for electrical vehicles, pumps, fans, valve control, centrifuges, machine tools, robots and industrial equipment. AFPM machines can also operate as small to medium power generators. Since a large number of poles can be accommodated, these machines are ideal for low speed applications, as for example, electromechanical traction drives hoists or wind generators. Moreover, AFPM have been today widely investigated in a large number of applications such as: submarine propulsion, airplane propulsion systems, wind energy, paper industry. The unique disc-type profile of the rotor and stator of AFPM machines makes it possible to generate diverse and interchangeable designs. AFPM machines can be designed as single air gap or multiple air gaps machines, with slotted, non-slotted or even totally ironless armature [1], [3], [4], [5].

II. MACHINE STRUCTURE OF CASE STUDY

AFPM machine topology that presented in this paper is Non-slotted TORUS machine (TORUS-NS). An idealized version of the machine structure is shown in Figure 1. The TORUS machine is a non-slotted, toroidal-stator, double-sided, axial-flux, disc-type, permanent magnet, brushless machine. Figure 1 shows the basic layout. A simple toroidal strip-wound laminated stator core carries a slot less toroidal

winding which may have any chosen number of phases. The rotor comprises two mild steel discs, one on each side of the stator, carrying axially-polarized magnets [6]. Use of the high-field permanent-magnet material Neodymium-Iron-Boron (NdFeB) for excitation enable quite high flux density to be achieved in the relatively large air-gap associated with the slotless winding [7]. The active conductor lengths are the radial portions facing the magnets. It is seen that the machine effectively comprises two independent halves, lying either side of the radial centreline. The name Torus was adopted to indicate the toroidal nature of both the stator core and the stator winding [6]. The geometry of the TORUS-NS machine is described in Figure 2 [8]. The three phase winding arrangement, magnet polarities and flux paths in the magnetic circuit in average diameter of the TORUS-NS machine are shown in Figure 3 [1].

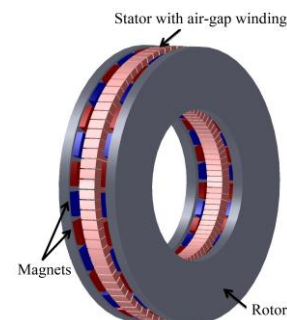


Figure 1. Axial flux TORUS type non-slotted surface mounted PM machine configuration (TORUS-NS).

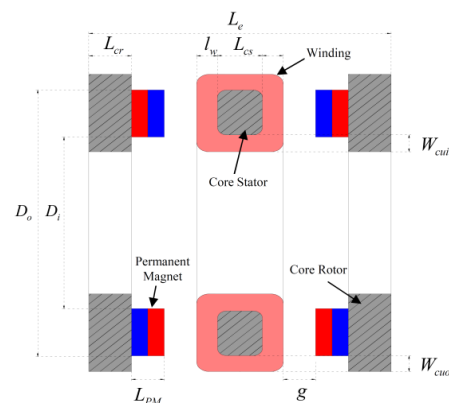


Figure 2. Definition of the geometrical parameters for the TORUS-NS AFPM machines [8]

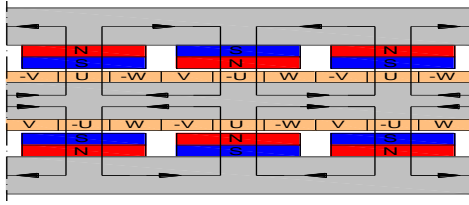


Figure 3. Three-phase winding, PM polarities and magnetic flux paths of a TORUS-NS machine [1].

III. INITIAL DESIGN OF TORUS-NS MACHINE

In this section performed initial design of TORUS-NS machine by use of certain algorithm. The selected values of principal design details are given in Table I. The overall specification for the direct-drive generator was 5 kW nominal demanded Power, 200 R.P.M nominal speeds [9].

TABLE I. SELECTED VALUES OF PRINCIPAL DESIGN DETAILS

Symbol	Quantity	Value	Unit
P_R	Nominal power	5000	[W]
m	Number of phase	3	-
V_{DC}	DC Voltage	210	[V]
f	frequency	46.67	[Hz]
n	Nominal speed	200	[rpm]
connection		wye	

TABLE II. ANALYTICALLY DESIGNED PARAMETER OF TORUS-NS AFPM MACHINE

Symbol	Quantity	Value	Unit
V_L	Line Voltage	219.05	[V]
V_p	Phase Voltage	126.47	[V]
p	Number of pole pair	14	-
A	Electrical Loading	10500	[A/m]
J	Current Density	7.8	[A/mm ²]
a_p	Number of parallel path	7	-
B_g	Air-gap peak flux density	0.74	[T]
λ	Diameter ratio	0.5745	-
K_p	Electrical power waveform factor	0.777	-
K_i	Current waveform factor	0.134	-
K_e	EMF factor	π	-
K_{cu}	Copper fill factor	0.33	-
μ_{rPM}	Magnetic recoil permeability	1.05	-
B_r	residual flux density of the PM material	1.17	[T]
B_{cr}	Flux density in the rotor core	1.17	[T]
K_d	Leakage flux factor	0.533	-
B_u	Specific magnetic loading	1.125	[T]
η	Efficiency	0.81	-
D_o	Outer Diameter	0.470	[m]
D_i	Inner Diameter	0.270	[m]
D_g	Average Diameter	0.370	[m]
g	Air-gap length (magnet to the winding)	0.0015	[m]
B_{cs}	Flux density in the stator core	1.245	[T]
L_{cs}	Axial length of the stator core	0.020	[m]
W_{cui}	Winding thickness at inner diameter	0.0055	[m]
W_{cuo}	Winding thickness at outer diameter	0.0032	[m]
W_{cu}	Winding thickness at inner diameter	0.0043	[m]
L_s	axial length of the stator	0.0288	[m]
L_{cr}	axial length of the rotor core	0.020	[m]
L_{PM}	PM length	0.0127	[m]
α_i	magnet width-to-pole pitch ratio	0.72	-

w_{PMg}	Magnet width in average diameter	0.0299	[m]
L_r	axial length of the rotor	0.0327	[m]
L_e	axial length of the machine	0.097	[m]
N_t	number of turns per phase	160	turn
I_{rms}	RMS phase current	12.71	[A]
l_w	axial thickness of the winding	0.0044	[m]
s_a	cross-section of a conductor	0.329	[m ²]
d_{str}	Strand wire diameter	0.71	[m]
L_i	effective length of the stack	0.1	[m]
L_{lav}	Average length of the armature turn	0.2576	[m]

IV. SIMULATION OF TORUS-NS MACHINE

In this section simulated TORUS-NS machine by means of FEM with mentioned parameter in table I and II. As mentioned before it is seen that the machine effectively comprises two independent halves, lying either side of the radial centerline. Measured view of TORUS-NS machine model for simulation is shown in Figure 4.

After drawing the model for simulation of TORUS-NS machine and attribution of the material for component of machine carry out mesh generation. Meshing of machine is shown in Figure 5.

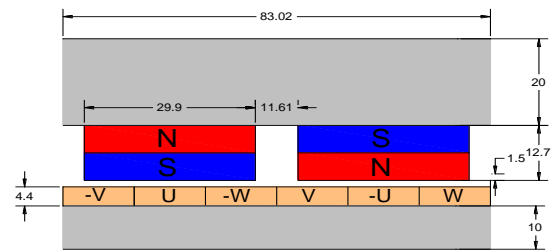


Figure 4. View of model for simulation of TORUS-NS machine.

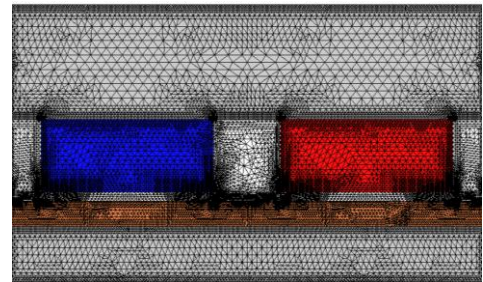


Figure 5. Meshing of TORUS-NS machine.

The magnetic flux lines for no-load condition are depicted in Figure 6.

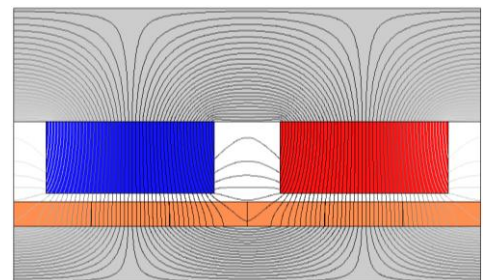


Figure 6. Magnetic flux lines for no-load condition of TORUS-NS machine.

The flux density distribution by means of vectors and direction of flux for no-load condition is depicted in Figure 7.

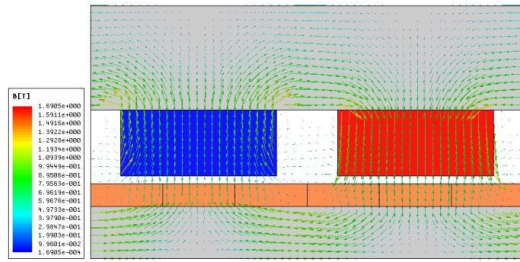


Figure 7. Flux density distribution by means of vectors and direction of flux for no-load condition.

The flux density distribution for no-load condition is depicted in Figure 8.

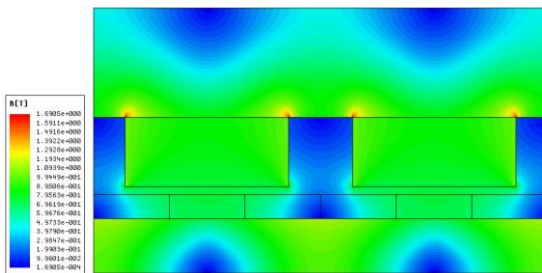


Figure 8. Flux density distribution for no-load condition of TORUS-NS machine.

Figure 9 shows the air-gap flux density over one pole using FEA. It can be seen from this curve that the maximum air-gap flux density is roughly 0.748 T and the average air-gap flux density was determined to be 0.61 T.

A flux density comparison between the sizing analysis results and FEA results on various parts of the TORUS-NS machine at no load is tabulated in Table III.

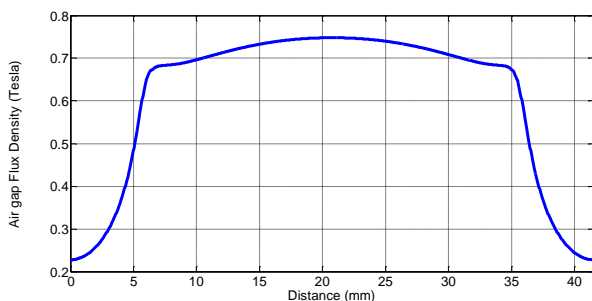


Figure 9. No load air-gap flux density of the TORUS-NS (at average diameter $D_g = (D_i + D_o)/2$).

TABLE III. FLUX DENSITY COMPARISON OF TORUS-NS MACHINE AT NO LOAD

Flux Density	B_{cs-max}	B_{cr-max}	B_{g-max}	B_{cs-avg}
FEM	1.123	1.09	0.748	0.61
Sizing eq.	1.245	1.17	0.748	0.60

It is seen that the FEA results are consistent with the results obtained from the sizing analysis except for the fact that maximum value of the stator flux density is a little lower than the value obtained from sizing analysis. The reason for this discrepancy is that the leakage flux is a bit higher because of the large air-gap which results in lower flux density in the stator core [10].

The magnetic flux density in the x (tangential) and y (normal) directions are shown in Figure 10.

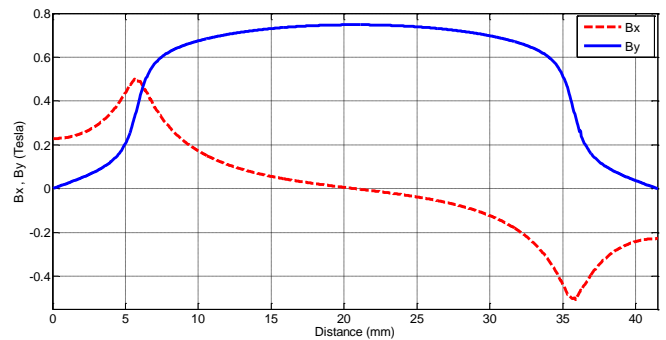


Figure 10. Magnetic flux density in the x (tangential) and y (normal) directions of TORUS-NS machine.

V. CONCLUSION

In this paper with selected values of principal design details Designed by use of a certain algorithm Parameter of TORUS-NS AFPM Machine. Then machine simulated by use of Finite Element Method (FEM). The FEA results are consistent with the results obtained from the sizing analysis that validates high precision of design algorithm studied in this paper.

APPENDIX

Equation of initial design algorithm:

- 1) Outer Diameter:

$$D_o = \left(\frac{4p P_R}{N_{stator} \pi K_e K_i K_p \eta B_g A f (1 - \lambda^2)(1 + \lambda)} \right)^{\frac{1}{3}} [m]$$

- 2) Inner diameter:

$$D_i = \lambda D_o [m]$$

- 3) Average air-gap diameter:

$$D_g = \frac{1 + \lambda}{2} D_o [m]$$

- 4) Flux density in the stator core

$$B_{cs} = 5.47 f^{-0.32} [T]$$

- 5) Axial length of the stator core

$$L_{cs} = \frac{B_g \pi D_o (1 + \lambda)}{B_{cs} 4p} [m]$$

- 6) Winding thickness at inner diameter

$$W_{cui} = \frac{\sqrt{D_i^2 + \frac{4A_s D_g}{K_{cu} J_s}} - D_i}{2} \quad [m]$$

- 7) Winding thickness at outer diameter

$$W_{cuo} = \frac{\sqrt{D_o^2 + \frac{4A_s D_g}{K_{cu} J_s}} - D_o}{2} \quad [m]$$

- 8) Axial length of the stator

$$L_s = L_{cs} + 1.6W_{cui} \quad [m]$$

- 9) Axial length of the rotor core

$$L_{cr} = \frac{B_u \pi D_o (1 + \lambda)}{B_{cr} 8p} \quad [m]$$

- 10) Permanent Magnet axial length

$$L_{PM} = \frac{\mu_{rPM} B_g}{B_r - \frac{K_f}{K_d} B_g} (g + W_{cu}) \quad [m]$$

- 11) Axial length of the rotor

$$L_r = L_{cr} + L_{PM} \quad [m]$$

- 12) Axial length of the machine

$$L_e = L_s + 2L_r + 2g \quad [m]$$

REFERENCES

- [1] Jacek F. Gieras, Rong-Jie Wang and Maarten J. Kamper, "Axial Flux Permanent Magnet Brushless Machines", Publisher: Springer; Second edition, 2008.
- [2] M. Aydin, S. Huang and T. A. Lipo, "Axial Flux Permanent Magnet Disc Machines: A Review", Research Report, University of Wisconsin-Madison 2004.
- [3] A. Bellara, Y. Amara, G. Barakat and P. Reghem, "Analytical Modeling of the Magnetic Field in Axial Flux Permanent Magnet Machines with Semi-Closed Slots at No Load" XIX International Conference on Electrical Machines - ICEM 2010, Rome
- [4] Fabrizio Marignetti, Giovanni Tomassi, Piergiacomo Cancelliere, Vincenzo Delli Colli, Roberto Di Stefano, Maurizio Scarano, "Electromagnetic and Mechanical design of a Fractional-slot-windings Axial-flux PM synchronous machine with Soft Magnetic Compound Stator", IEEE 2006.
- [5] A. Parviainen, J. Pyrhönen, M. Niemelä, "AXIAL FLUX INTERIOR PERMANENT MAGNET SYNCHRONOUS MOTOR WITH SINUSOIDALLY SHAPED MAGNETS" ISEF 2001 - 10th International Symposium on Electromagnetic Fields in Electrical Engineering Cracow, Poland, September 20-22, 2001.
- [6] B.J. Chalmers, Wu Wei, E. Spooner, "An Axial-Flux Permanent-Magnet Generator for a Gearless Wind Energy System", IEEE Int. Conf. on Power Electronics, Drives and Energy Systems for Industrial Growth, PEDESP6, New Delhi, pp. 610-616.
- [7] E. SPOONER, B.J. CHALMERS, M.M. El Missiry, WU WEI and A.C. RENFREW, "MOTORING PERFORMANCE OF THE TOROIDAL PERMANENT MAGNET MACHINE "TORUS"", University of Manchester Institute of Science and Technology, UK University of Zimbabwe, Zimbabwe.
- [8] F. Libert, "Design, Optimization and Comparison of Permanent Magnet Motors for a Low-Speed Direct-Driven Mixer", Licentiate Thesis, Royal Institute of Technology, Stockholm 2004.
- [9] F. Caricchi, B.J. Chalmers, F. Crescimbeni, E. Spooner "Advances in the Design of TORUS Machines", IEEE, pp. 516-522 Vol. 2, 1-3 Dec.1998.
- [10] M. Aydin, S. Huang and T. A. Lipo, "Design and 3D Electromagnetic Field Analysis of Non-slotted and Slotted TORUS Type Axial Flux Surface Mounted Permanent Magnet Disc Machines," International Electrical Machines and Drives Conference, IEEE 2001, Boston.



Hassan Moradi received the B.Sc. degree in electrical engineering from Shahid Rajaee University, Tehran, Iran, in 2001 and the M.Sc. degree in the same field from Shahrood University of Technology in 2012. His research activities are mostly on design and modeling of electrical machines.



Ahmad Darabi received the B.Sc. degree in electrical engineering from the University of Tehran, Tehran, Iran, in 1989 and the M.Sc. degree in the same field from Ferdowsi University, Mashhad, Iran, in 1992. He obtained the Ph.D. degree with the Electrical Machine Group, Queen's University, Belfast, U.K., in 2002. He is now an associated professor and has been with the Faculty of Electrical and Robotic Engineering, Shahrood University of Technology, Shahrood, Iran, since 1993. His research activities are focussed mostly on design, modelling, and manufacturing of miniature electrical machines and generating sets.